# Binding and internalization of NGR-peptide-targeted liposomal doxorubicin (TVT-DOX) in CD13-expressing cells and its antitumor effects

Seema V. Garde[a], André J. Forté[a], Michael Ge[a], Eugene A. Lepekhin[a], Chandra J. Panchal[a], Shafaat A. Rabbani[b] and Jinzi J. Wu[a]

**In an effort to develop new agents and molecular targets for the treatment of cancer, aspargine-glycine-arginine (NGR)-targeted liposomal doxorubicin (TVT-DOX) is being studied. The NGR peptide on the surface of liposomal doxorubicin (DOX) targets an aminopeptidase N (CD13) isoform, specific to the tumor neovasculature, making it a promising strategy. To further understand the molecular mechanisms of action, we investigated cell binding, kinetics of internalization as well as cytotoxicity of TVT-DOX *in vitro*. We demonstrate the specific binding of TVT-DOX to CD13-expressing endothelial [human umbilical vein endothelial cells (HUVEC) and Kaposi sarcoma-derived endothelial cells (SLK)] and tumor (fibrosarcoma, HT-1080) cells *in vitro*. Following binding, the drug was shown to internalize through the endosomal pathway, eventually leading to the localization of doxorubicin in cell nuclei. TVT-DOX showed selective toxicity toward CD13-expressing HUVEC, sparing the CD13-negative colon-cancer cells, HT-29. Additionally, the nontargeted counterpart of TVT-DOX, Caelyx, was less cytotoxic to the CD13-positive HUVECs demonstrating the advantages of NGR targeting *in vitro*. The antitumor activity of TVT-DOX was tested in nude mice bearing human prostate-cancer xenografts (PC3). A significant growth inhibition (up to 60%) of PC3 tumors *in vivo* was observed. Reduction of tumor vasculature following treatment with TVT-DOX was also apparent. We further compared the efficacies of TVT-DOX and free doxorubicin in the DOX-resistant colon-cancer model, HCT-116, and observed the more pronounced antitumor effects of the TVT-DOX formulation over free DOX. The potential utility of TVT-DOX in a variety of vascularized solid tumors is promising. *Anti-Cancer Drugs* 18:1189–1200 © 2007 Wolters Kluwer Health | Lippincott Williams & Wilkins.**

**Anti-Cancer Drugs** 2007, **18**:1189–1200

**Keywords: aspargine-glycine-arginine (NGR), CD13, NGR-liposomal doxorubicin, vascular targeting**

[a]Ambrilia Biopharma Inc., Chemin Du Golf, Verdun and [b]Department of Medicine, Physiology and Oncology, McGill University Health Centre, Montreal, Quebec, Canada

Correspondence to Dr Seema V. Garde, PhD, Ambrilia Biopharma Inc., 1000 Chemin Du Golf, Verdun, Quebec, Canada H3E 1H4
Tel: +1 514 732 3219; fax: +1 514 751 2502;
e-mail: sgarde@ambrilia.com

**Received** 19 December 2006 **Revised form accepted** 29 May 2007

## Introduction

The traditional approach to cancer therapy has focused on targeting and destroying cancer cells. Direct access to cancer cells is, however, often restricted; this has led to the limited success of various drugs. To overcome this, recent strategies have attempted to target tumor vasculature instead of the cancer cells directly [1,2]. Suppression of new blood vessel formation (antiangiogenic therapy) and destruction of established tumor vasculature (antivascular therapy) have both been explored. The lack of functional vasculature leads to tumor starvation and eventually to regression [3]. Thus, targeted drug therapy to tumor vasculature has emerged as one of the most promising approaches for the treatment of cancer.

Compared to normal blood vessels, tumor vasculature has an abnormal wall structure and branching patterns with uneven diameters [4]. Endothelial cells in the angiogenic vessels within solid tumors express several proteins that are absent or are barely detectable in established blood vessels [5]. Such molecular markers include integrin $\alpha_v\beta_3$ and $\alpha_v\beta_5$ [6], aminopeptidase N (APN/CD13) [7], vascular endothelial growth factor receptor (VEGFR) [8], matrix metalloproteinase (MMP), proteoglycan (NG2) [9], and prostate-specific membrane antigen (PSMA) [10]. Some of these are used as targets for tumor-specific delivery of therapeutic agents [11–14]. Among the various new targeting ligands identified, peptides containing the aspargine–glycine–arginine (NGR) motif have been shown to home into the tumors by binding to CD13 [7]. Although there are several subpopulations of CD13 [15], which are relatively widely distributed in the body, only one isoform is believed to be the receptor for the NGR peptide. This isoform was shown to be expressed exclusively in angiogenic vessels, such as the neovasculature found in tumor tissues [16,17]. Ever since the discovery of the NGR tumor-homing peptide, researchers have used this ligand for the delivery of various antitumor compounds such as chemotherapeutic drugs [12], apoptotic peptides [18], viral particles [19], cytokines [20] and liposomes [21] to

0959-4973 © 2007 Wolters Kluwer Health | Lippincott Williams & Wilkins

tumor vessels through its binding to the CD13-specific isoform.

A potential candidate for NGR-targeted delivery is doxorubicin (DOX). It is a widely used chemotherapeutic agent with antineoplastic properties, which exhibits potent effects on a wide spectrum of solid tumors and hematopoietic malignancies. A continued effort is, however, being made to improve its targeted delivery, to minimize the serious systemic side effects caused by the drug [22–24]. Incorporation of DOX inside polyethyleneglycol (PEG)-coated liposomes (stealth liposome) significantly prolonged drug circulation time, as it avoids the reticuloendothelial removal system [25–27]. Stealth-liposomal DOX (Caelyx; Mayne Pharma, Montreal, Canada) is now commercially available for the treatment of a variety of cancers [28–30]. Further development for stealth-liposomal DOX was to combine it with an NGR peptide [NGR-SL (DXR)], which successfully enhanced its therapeutic index in a neuroblastoma mouse model [21]. The NGR-targeted liposomal formulation used in the aforementioned study was, however, prepared at the laboratory scale. It is not compatible with the large-scale Good Manufacturing Practice (GMP) preparation that would be required for preclinical studies and subsequent human clinical trials.

In this communication, we evaluated the efficacy of NGR-targeted liposomal doxorubicin (TVT-DOX), manufactured in a GMP-type environment in-vitro cellular binding, internalization and a functional cytotoxicity assay. We show the specific binding of TVT-DOX to CD13-expressing cells. The kinetics of TVT-DOX internalization, intracellular release and nuclear uptake of DOX are observed in various CD13-expressing cells by fluorescent microscopy. As the NGR-tumor targeted delivery can be potentially effective in any type of vascularized solid tumor irrespective of histologic origin, we sought to test the efficacy of TVT-DOX in the prostate-cancer PC3 mouse xenograft model. TVT-DOX was able to reduce PC3 tumor growth and vascularization *in vivo*. We further extended our study to compare the efficacies of TVT-DOX and free DOX in DOX-resistant colon cancer model, HCT-116.

## Materials and methods

### Reagents

The NGR peptide (G**NGR**GGVRSSSRTPSDKYC) was synthesized by the American Peptide Company(Sunnyvale, California, USA). DOX hydrochloride (DOX HCl) and pegylated liposomal DOX, (Caelyx) were purchased from Mayne Pharma (Montreal, Quebec, Canada) and Alza Corporation (Menlo Park, California, USA), respectively. Vectastain Elite Mouse IgG ABC kit and Vecta Shield mounting medium with propidium iodide were from Vector Laboratories (Burlingame, California, USA). The MTS cell-proliferation assay kit was from Promega (Madison, Wisconsin, USA). The Lyso Tracker Green DND-26 was from Molecular Probes (Eugene, Oregon, USA). The Tris–acetate precast gels (3–8%) were from Invitrogen (Burlington, Ontario, Canada) and the enhanced chemiluminescence kit (ECL) was from Santa Cruz Biotechnology (Santa Cruz, California, USA). All other reagents of biochemical and molecular biology grades were obtained from Sigma-Aldrich (Oakville, Ontario Canada).

### Antibodies

The mouse antihuman CD13 antibody (clone WM15), rat antimouse CD31 antibody, and isotype-matched control mouse IgG1 and rat IgG2a were from BD Pharmingen (Franklin Lakes, New Jersey, USA). The anti-human CD13 antibody (clone 3D8) for Western blotting was from Santa Cruz Biotechnology.

### Aspargine–glycine–arginine (NGR)-targeted liposomal doxorubicin synthesis

TVT-DOX was manufactured by Northern Lipids (Vancouver, Canada) by means of proprietary technology. Briefly, liposomes were composed of hydrogenated soybean phosphatidylcholine cholesterol, 1,2-distearoyl-*sn*-glycero-3-phosphoethanolamine-*N*-[PEG(2000)] conjugate (DSPE-PEG) and DSPE-PEG-NGR peptide conjugate. Liposome components were dissolved in solvent and diluted by ammonium sulfate buffer. The diluted lipids were extruded to form unilamellar vesicles, which were then ultrafiltered to remove external ammonium sulfate and create a transmembrane gradient. Following the ultrafiltration of lipids, up to 2 mg/ml DOX HCl was loaded into liposomes in response to the transmembrane pH gradient. Loaded liposomes were sterile-filtered and aseptically sealed in vials.

### Cell lines and cell culture

Human umbilical vein endothelial cells (HUVEC) were purchased from Clonetics (East Rutherford, New Jersey, USA) and maintained in endothelial cell basal medium-2 (EBM-2; Clonetics). Human prostate cancer cells (PC3), fibrosarcoma (HT-1080) and colon cancer cells (HT-29) were purchased from the American Type Culture Collection (ATCC, Rockville, Maryland, USA) and maintained in culture media as per ATCC recommendations. The AIDS-related Kaposi sarcoma-derived endothelial cell line (SLK) was from the National Institutes of Health (NIH) AIDS Research and Reference Reagent Program (Germantown, Maryland, USA) and grown in RPMI supplemented with 10% fetal bovine serum.

### Immunofluorescent detection of aminopeptidase N (CD13) expression

To examine cellular surface expression of the CD13 marker, HT-1080, HUVEC, SLK and HT-29 cells were

plated into two-chambered slides at a density of 50 000 cells/well. After overnight incubation, cells were fixed in 4% paraformaldehye for 10 min. Cells were then washed in phosphate-buffered saline (PBS), blocked in normal horse serum (1%) and then incubated with an anti-CD13 monoclonal antibody (WM15) at 2 μg/ml. Biotinylated anti-mouse IgG (2 μg/ml) was used as the secondary antibody, followed with fluorescein-labeled streptavidin (Vector Laboratories). Slides were mounted with Vecta Shield solution containing propidium iodide. An isotype-matched antibody (IgG2) was used as negative control at the same dilution as the anti-CD13 primary antibody.

#### Detection of aminopeptidase N (CD13) expression by Western blotting

For Western blot analysis of CD13, various cells grown in 75-$cm^2$ culture flasks were pelleted and resuspended in lysis buffer [10 mmol/l Tris–HCl (pH 7.2) containing 150 mmol/l NaCl, 1% (v/v) Triton X-100, 0.1% (v/v) SDS, 1% deoxycholate and 5 mmol/l EDTA, supplemented with complete, mini protease inhibitors (Roche Diagnostics, Laval, Quebec, Canada)]. The cell debris was removed by centrifugation (10 000 rpm at 4°C for 10 min) and the protein concentration was determined with the bicinchoninic acid protein assay (Pierce, Rockford, Illinois, USA). Samples of cell extracts containing 40 μg of protein were loaded on SDS–PAGE gels and transferred to polyvinylidene fluoride membrane filters (Invitrogen). CD13 protein was detected with anti-CD13 antibody (1:100) and peroxidase-conjugated secondary antibody (Jackson Immuno Research Labs, West Grove, Pennsylvania, USA). The antigen–antibody complexes on the membranes were visualized with ECL Western Blotting Detection System. Actin was also detected with anti-β-actin as an internal control and used for normalization purposes in the densitometric analysis.

#### Fluorescent detection of cellular binding of various doxorubicin formulations

The cellular binding of TVT-DOX, Caelyx and DOX was evaluated by incubating the HT-1080, HUVECs, SLK and HT-29 cells grown in chamber slides with the above formulations of DOX at 20 μg/ml for 1 h at 4°C in Hank's balanced salt solution (HBSS). After incubation with the drugs, cells were washed with HBSS, mounted and observed for DOX fluorescence under a Nikon microscope using a triple-band pass filter. For competition experiments, cells were incubated with either TVT-DOX alone or TVT-DOX with 150-fold excess free NGR peptide for 1 h at 4°C.

For a quantitative evaluation of the TVT-DOX, Caelyx and free DOX on cellular binding, cells were detached from flasks with 3 mmol/l EDTA–PBS, counted and put into microfuge tubes (75 000–300 000 cells/tube, 4 tubes/cell line). Cells were spun down at 200*g* for 5 min (4°C) and washed once with 1 ml of cold PBS. Cells were then resuspended in 500 μl of TVT-DOX, Caelyx or free DOX diluted in PBS at 20 μg/ml. Control cells were resuspended in PBS alone. Tubes with cells were placed on a rocker for 30 min at 4°C for drug binding. After incubation, cells were spun down as before and washed once with 1 ml of cold PBS. At these low centrifugation speeds required to maintain intact cells, the drug formulations remained in suspension and were removed when aspirating the supernatant. Cells were finally resuspended in 100 μl of PBS with 5% Triton X-100. This breaks up not only the cells, but also the liposomes, liberating the encapsulated DOX. Using an FL-600 fluorometer, fluorescence inherent to DOX was used to quantify the binding of drug formulations to cells. Fluorescence readings were taken with an excitation wavelength of 460 nm and an emission wavelength of 645 nm. Values were then normalized using the initial cell number to estimate the amount of drug binding/cell.

#### Internalization of aspargine–glycine–arginine (NGR)-targeted liposomal doxorubicin

To study the kinetics of internalization, HT-1080, SLK and HT-29 cells were incubated in HBSS with 20 μg/ml TVT-DOX at 37°C for various times (15, 30 and 60 min), and observed for DOX fluorescence under fluorescent microscope.

For studies on endocytic transport of encapsulated drug, SLK cells were pre-incubated for 1 h at 37°C with or without bafilomycin A1 at a concentration of 1 μmol/l before addition of 20 μg/ml TVT-DOX. After further incubation for 2 h at 37°C, cells were washed extensively and observed under fluorescent microscope.

To further study the intracellular fate of the liposomes containing TVT-DOX, we carried out colocalization studies using Lyso Tracker Green DND-26 and TVT-DOX. The SLK cells grown on chamber slides were washed with PBS and incubated in 1 ml of HBSS supplemented with 200 mmol/l Lyso Tracker Green and 20 μg/ml TVT-DOX at 37°C. After 1 h, the cells were washed with fresh HBSS and observed using fluorescence microscope under green and triple-band pass filters.

#### Measurement of free doxorubicin in aspargine–glycine–arginine (NGR)-targeted liposomal doxorubicin and Caelyx preparations by high-performance liquid chromatography/ultraviolet analysis

To determine the amount of free DOX in the liposomal drug preparations, aliquots of TVT-DOX and Caelyx were added onto Microcon-10 filters and centrifuged at 8000*g* for 30 min at 4°C. The free DOX (flowthrough) obtained from the above step was compared with the total amount of DOX in the original liposomal formulations. Detection and quantification of DOX was performed by high-performance liquid chromatography (Agilent 1100) using

a reversed-phase column (Zorbax SB-C18, 2.1 × 50 mm, 5 μm; Agilent, Santa Clara, California, USA). The detector was set at 487 nm. A gradient elution was used, consisting initially of 80% water with 0.1% formic acid and 20% acetonitrile with 0.1% formic acid; this was brought to 100% acetonitrile with 0.1% formic acid in 5 min and held for 2 min. The mobile phase was then brought back to the initial composition in 1 min and equilibrated for 4 min. Flow rate was 0.3 ml/min.

### In-vitro cytotoxicity assays

HUVEC and HT-29 cells were seeded in 96-well plates at a density of $10^3$ cells/well (in triplicates). Twenty-four hours later, cells were washed once with HBSS and exposed for 1 h to various concentrations of free DOX, TVT-DOX, empty liposomes or Caelyx diluted in HBSS at 37°C. The highest tested dose of DOX for the liposomal preparations was 200 μg/ml, which contained approximately 1 mg/ml lipids. The cells were then washed twice and incubated further in drug-free complete medium. Cell growth was assessed after 48 h by MTS assay and the optical densitys were measured at 490 nm. Cells that did not receive any drug (control) were considered as having 100% cell growth and growth from treated cells was compared with this value (percent growth versus control).

### Animal protocols

#### *Prostate cancer PC3 xenograft model*

Male athymic nude mice (6–8 weeks old, 25–28 g) were purchased from Charles River (St-Constant, Quebec, Canada); sterile water and food were supplied *ad libitum*. After a week's quarantine, PC3 cells ($8 \times 10^6$) in serum-free culture media were injected subcutaneously in both flanks of six mice. Tumors grown from this inoculum were excised at approximately 200 $mm^3$ and minced into 2–3 $mm^3$ for trocar implantation into recipient mice. Xenografts were allowed to grow for 10 days before treatment was initiated. Before the first treatment, all animals were identified by ear notch, weighed and randomized into different groups (8 animals/group). Experimental animals received 1, 3 and 6 mg/kg of TVT-DOX once a week for 6 weeks through the tail vein. Control animals received PBS alone as vehicle control. All the animals were monitored weekly for their tumor development. Tumor volumes were estimated weekly with length ($l$) and width ($w$) caliper measurements, using the following equation: $lw^2/2$. Every animal was weighed once a week throughout the study to determine any adverse effects of the drug. Treatment was stopped after the sixth injection and animals were further monitored for 3 weeks before being killed. At termination, body weight, tumor volume and tumor weight were recorded.

#### *Colon cancer HCT-116 model*

Female athymic nude mice of 7–8 weeks old were from Harlan (Indianapolis, Indiana, USA). After acclimatization for a week, they were injected with HCT-116 colon-cancer cells ($5 \times 10^6$ tumor cells subcutaneously in the right flank of each animal). The growth of tumors was monitored and as the average size approached 80–120 $mm^3$, the animals were segregated into three groups each consisting of 10 mice. TVT-DOX (5 mg/kg) and free DOX (5 mg/kg) were administered intravenously once a week for 5 weeks. Tumor volumes were measured twice weekly as described in the PC3 model. Each animal was euthanized when its tumor reached the endpoint size of 1500 $mm^3$. Treatment outcome was assessed by calculating the percentage tumor-growth inhibition in the treated groups compared with controls, at the time the first animal reached the endpoint size.

### Histologic analysis

To study the tumor vascularization following treatment with TVT-DOX, an additional group of PC3-tumor-bearing animals received four intravenous injections of 6 mg/kg/week of TVT-DOX (control group received PBS alone as vehicle control). Animals were killed 24 h after the fourth injection. Tumors were snap frozen and cryosections (6 μm) were stained using monoclonal antibodies against CD31. Briefly, sections were fixed in chilled acetone, washed in PBS and incubated in 1% normal rabbit serum before treatment with the primary antibody (rat anti-mouse CD31) at 1:50 dilution overnight at 4°C. Biotinylated rabbit anti-rat IgG (Vector Laboratories) was used as the secondary antibody at 1:200 for 30 min at room temperature. The sections were further incubated with horseradish peroxidase–streptavidin (Vector Laboratories) for 30 min and subsequently developed with 3,3′-diaminobenzidine tetrahydrochloride (Sigma-Aldrich). Slides were counterstained with hematoxylin, dehydrated in alcohol and mounted with cytoseal-60.

### Computer-assisted image analysis

Computer-assisted image analysis was carried out to quantify positive immunostaining of CD31. Briefly, images of stained sections were photographed with a Leica digital camera and processed using BioQuant image analysis software, version 6.50.10 (BioQuant Image Analysis, Nashville, Tennessee, USA). The threshold was set by determining the positive staining of control sections and was used to automatically analyze all the recorded images of all the samples that were stained in the same session under identical conditions. The area of stained regions was calculated automatically by the software in each microscopic field. Pixel counts of the immunoreaction product were calculated automatically and were given as total density of the integrated immunostaining over a given area.

### Statistical analysis

Results are expressed as the means ± SE, and the statistical significance of differential findings between

experimental groups and controls was determined by Student's *t*-test. $P < 0.05$ was considered to be significant.

## Results

### Quantification of free doxorubicin in liposomal drug formulations

Quantification of free DOX in TVT-DOX and Caelyx formulations was performed for the quality-control purposes. Concentrations of free DOX were 0.4 and 0.2%, respectively, indicating no significant leakage of DOX from either formulation.

### Immunofluorescent detection of aminopeptidase N (CD13) expression

Fluorescent-microscopy analysis indicated that CD13 was expressed on the cell surface of HT-1080, HUVEC, and SLK cells, whereas HT-29 cells were negative (Fig. 1a, e, i and m, respectively). Visual assessment of the immunostaining suggested various levels of CD13 expression: HT-1080 > HUVEC > SLK. This assessment was well correlated with the results of Western blotting and the quantitative densitometric analysis of CD13 expression in these cells (Fig. 2a).

### Specific binding of aspargine–glycine–arginine (NGR)-targeted liposomal doxorubicin on aminopeptidase N (CD13)-positive cells

We tracked the red fluorescence of DOX molecules when the cells were incubated with TVT-DOX, Caelyx and free DOX at 4°C for 1 h (cell binding assay). Results revealed TVT-DOX binding on cell membranes of HT-1080, HUVEC and SLK cells as indicated by red fluorescence on the cell surface (Fig. 1b, f and j). The CD13-negative cell line HT-29 (Fig. 1n) did not show DOX fluorescence, suggesting that binding of TVT-DOX is related to CD13 expression.

Nontargeted Caelyx did not significantly bind to any of the cells (Fig. 1c, g, k and o), whereas an influx of the free DOX was observed directly into the nuclei of all tested cell lines (Fig. 1d, h, l and p). Quantitative measurement of DOX fluorescence signal as indicated in Fig. 2b correlated to some extent with the visual observations of DOX fluorescence on these cells. It should be noted that, when observations are made under the microscope, the liposomal DOX signal (with or without the NGR peptide) might be partially quenched because the DOX is inside the liposomes. For the quantitative measurements of binding, Triton-X-100 is added to break up the liposomes, to liberate the DOX and increase the signal.

Further, the specificity of TVT-DOX binding was tested with or without addition of 150-fold excess NGR peptide on the SLK cells for 1 h at 4°C. DOX fluorescence observed on the cell surface of SLK cells (Fig. 3a) was inhibited by addition of excess NGR peptide (Fig. 3b), suggesting that the NGR peptide was responsible for the binding of the drug to SLK cells.

### Kinetics of aspargine–glycine–arginine (NGR)-targeted liposomal doxorubicin internalization

To study the kinetics of drug internalization, we chose three cell lines with various levels of CD13 expression: high (HT-1080), intermediate (SLK) and no CD13 (HT-29), as seen from their immunostaining intensities (Fig. 1a, i and m, respectively). The kinetics of cellular drug binding, internalization, intracellular release of DOX from the liposomes and nuclear uptake varied from one cell line to another. The high CD13-expressing cell line HT-1080 exhibited intense fluorescence of DOX not only on the cell membrane but also internalized within the cell, within 15 min of incubation with TVT-DOX. As seen in Fig. 4a, the DOX fluorescence was visible at the periphery of the nuclei of the HT-1080 cells after 15 min of incubation. At 30 min, further increase in accumulation of the drug was observed in most of the cells (Fig. 4b). In a few cells, the drug had already gained entry into the nucleus, indicating the release of DOX from the liposomes. The accumulation of the drug in cytoplasm showed a more punctuate pattern than the drug that entered the nuclei. After 60 min of incubation with TVT-DOX, almost all the cells showed nuclear localization of DOX (Fig. 4c). In the intermediate CD13-expressing SLK cells, a similar binding/internalization pattern (Fig. 4d–f) to the HT1080 cells was observed, except that there was some delay. After 60 min, only a few SLK cells displayed DOX nuclear uptake, as was the case for the HT1080 cells after 30 min. As for the CD13-negative HT-29 cells, they displayed neither binding (see Fig. 1n) nor internalization of the drug (data not shown), even after 60 min. These results suggest that the kinetics of binding, internalization, and nuclear uptake of TVT-DOX is correlated with the amount of CD13 expression by the cells. In contrast, the nontargeted pegylated liposomal DOX, Caelyx, showed no internalization with any of these cell lines after 1 h of incubation at 37°C (data not shown).

### Bafilomycin A1 inhibits endosomal trafficking of internalized aspargine–glycine–arginine (NGR)-targeted liposomal doxorubicin

To investigate the influence of bafilomycin A1 on endocytic transport of the drug in SLK cells, we incubated the cells with or without 1 μmol/l bafilomycin for 1 h, followed by the addition of 20 μg/ml TVT-DOX (see Material and methods). Our results indicated that in control cells, DOX was visible in the perinuclear areas (a characteristic of late endosomes) as well as in cell nuclei (DOX liberated from the liposomes) (Fig. 5a). In the bafilomycin-treated cells, DOX fluorescence was quite weak and diffused, suggesting that the preincubation of cells with bafilomycin resulted in inhibition of late endosome formation, which prevented the liberation of the drug from liposomes (Fig. 5b). A further confirmation

**Fig. 1**

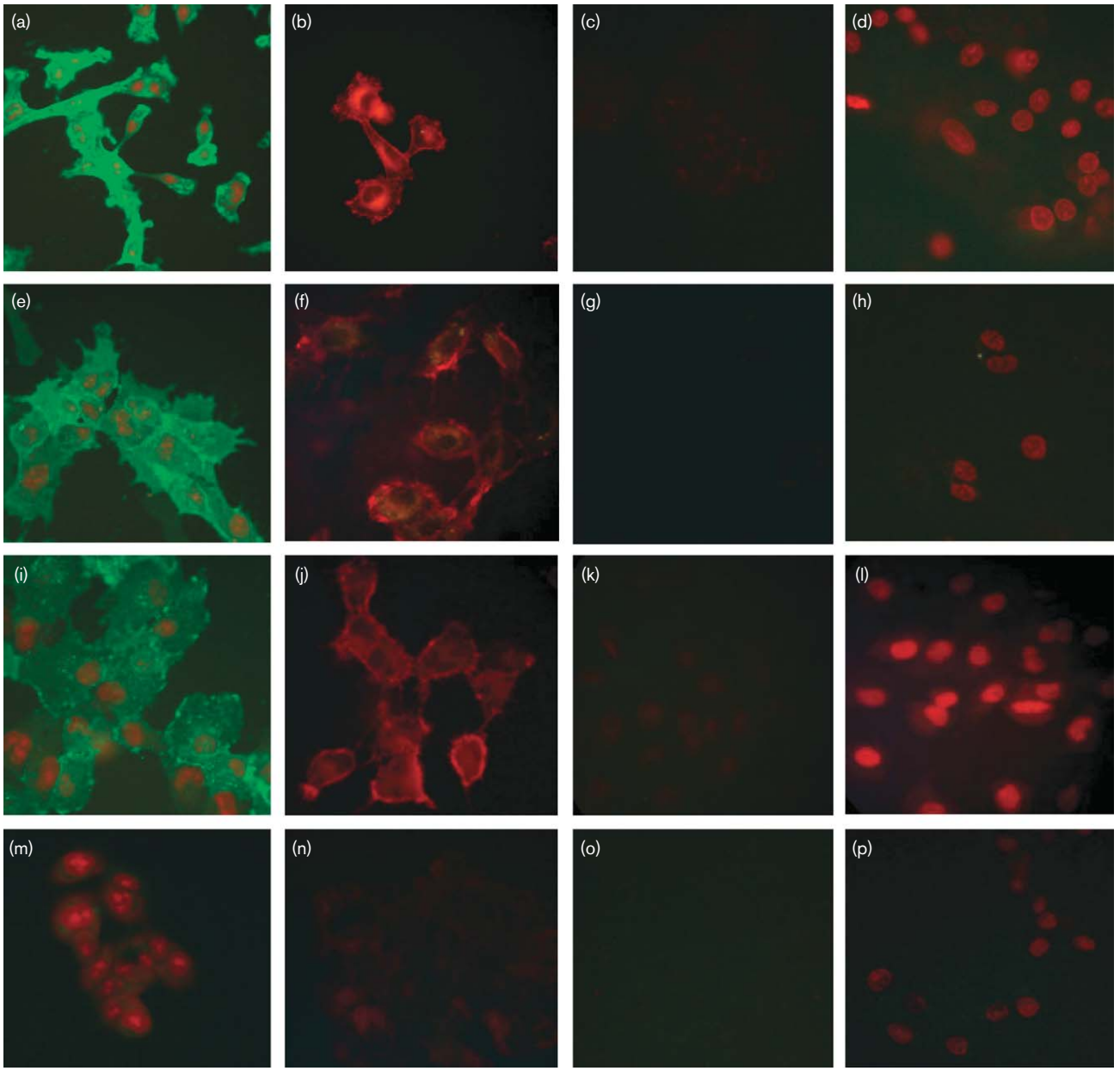


Aspargine–glycine–arginine (NGR)-targeted liposomal doxorubicin (TVT-DOX) binds to aminopeptidase N (CD13)-expressing cells *in vitro*: HT-1080 cells (a–d), human umbilical vein endothelial cells (e–h), Kaposi sarcoma-derived endothelial (SLK) cells (i–l) and HT-29 cells (m–p). The cells were incubated with a monoclonal antibody (WM15) to evaluate the expression of CD13 (a, e, i and m). Cells were incubated with 20 μg/ml of various doxorubicin (DOX) formulations: TVT-DOX (b, f, j and n), Caelyx (c, g, k and o) and free DOX (d, h, l and p). Incubation with drug at 4°C for 1 h, washing and evaluation for DOX fluorescence by fluorescent microscopy. Original magnification × 500.

on the intracellular fate of TVT-DOX through the endosome/lysosome pathway was obtained by incubating the cells with a lysosomal marker (Lyso Tracker Green DND-26) and TVT-DOX. Accumulation of green fluorescence due to Lyso Tracker Green in lysosomes (Fig. 6a) and red fluorescence of TVT-DOX due to DOX (Fig. 6b) in the same cellular area indicates their colocalization.

### In-vitro functional cytotoxicity assays

The efficient binding, internalization, and nuclear localization of TVT-DOX led us to reason that a pulse treatment of 1 h with TVT-DOX would be sufficient for the capture of the drug on CD13-expressing HUVECs; in contrast, Caelyx should be washed off. A functional cytotoxicity assay can then demonstrate the increased killing by the targeted drug. We also explored the

**Fig. 2**

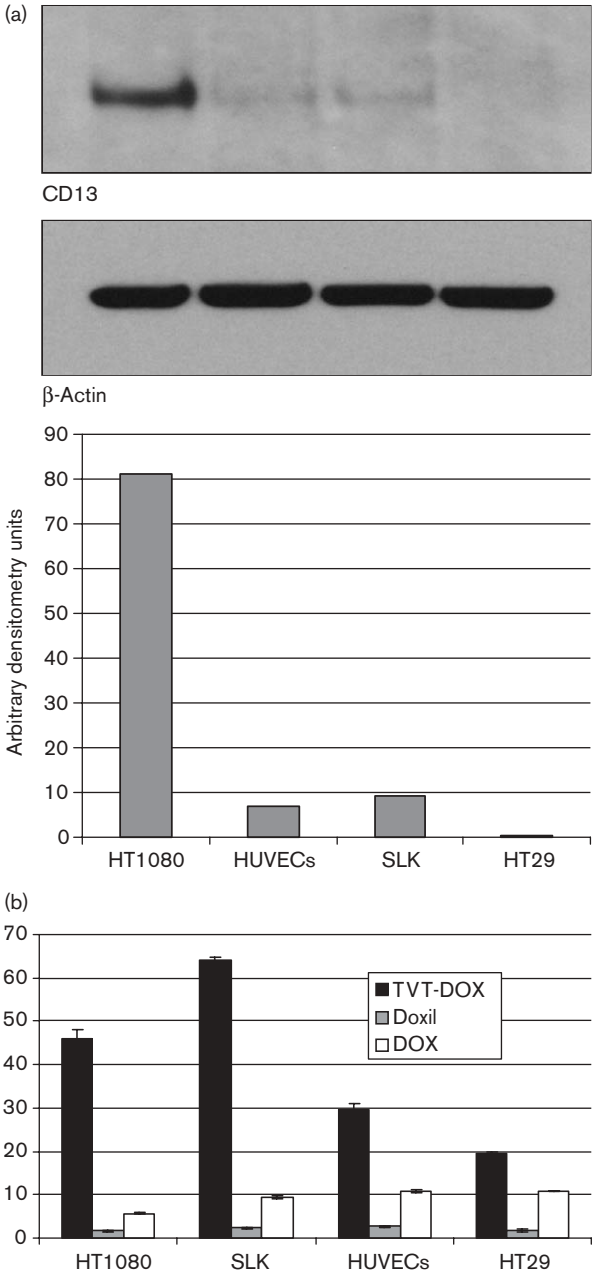


Quantitative evaluation of aminopeptidase N (CD13) expression and aspargine–glycine–arginine (NGR)-targeted liposomal doxorubicin (TVT-DOX) cellular binding: HT1080, Kaposi sarcoma-derived endothelial (SLK), human umbilical vein endothelial cells (HUVECs) and HT29 cell lysates were run on 3–8% Tris–acetate gel and Western blot analysis for CD13 (a) was carried out as described in Materials and methods. For the TVT-DOX cellular binding (b), cells were incubated with TVT-DOX, Caelyx and free DOX for 30 min at 4°C (20 μg/ml). Inherent DOX florescence was measured in the fluorometer after addition of Triton X-100 (460 nm excitation, 645 nm emission).

response of these drugs on CD13-negative HT-29 cells to confirm the selectivity of TVT-DOX toward CD13-expressing cells. As seen in Fig. 7a, growth inhibition of TVT-DOX-treated HUVEC cells was superior to those

**Fig. 3**

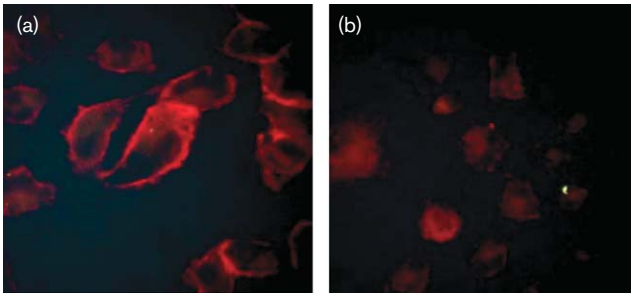


Specific binding of aspargine–glycine–arginine (NGR)-targeted liposomal doxorubicin (TVT-DOX) on Kaposi sarcoma-derived endothelial (SLK) cells: SLK cells grown in chambered slides were incubated with 20 μg/ml TVT-DOX alone (total binding) or TVT-DOX with 150-fold excess free NGR peptide for 1 h at 4°C. The cells were washed with phosphate-buffered saline (PBS) and evaluated for DOX fluorescence under fluorescent microscopy. Original magnification × 500

treated with nontargeted Caelyx. At 200 μg/ml of DOX, the targeted drug killed 81% of cells, whereas the nontargeted counterpart only killed 38%. As expected, the direct localization of free DOX to the nucleus led to high levels of cytotoxicity even at relatively low concentrations (Fig. 7a). Empty liposomes with the NGR peptide on their surfaces did not inhibit HUVEC growth. Free DOX exhibited high levels of cytotoxicity on the CD13-negative cells (HT-29); however, neither of the liposomal formulations did (NGR-targeted and nontargeted) (Fig. 7b). These results suggest that the role of the NGR peptide-mediated drug binding, internalization, and delivery is crucial for liposomal DOX cytotoxicity in CD13-expressing cells.

### In-vivo antitumor activity of aspargine–glycine–arginine (NGR)-targeted liposomal doxorubicin

#### *Prostate-cancer (PC3) model*

The efficacy of TVT-DOX in inhibiting PC3 tumor growth was tested in an athymic nude-mouse model. Weekly administration of TVT-DOX at 1, 3 and 6 mg/kg, starting 10 days after tumor implantation for 6 weeks, resulted in a dose-dependent growth inhibition of PC3 tumors (Fig. 8a). When comparing with control animals, there was a significant reduction in tumor weight at termination (day 67) in the treated groups [35, 50 and 63% tumor-weight reduction for animals treated with 1, 3 and 6 mg/kg/week of TVT-DOX, respectively (Fig. 8b)]. Weekly body-weight measurements depicted a significant weight loss in the 6-mg/kg/week group during the treatment period, suggesting toxicity of the drug at this dose (Fig. 8c). The animals, however, regained much of the weight when the treatment was discontinued. The body weights of the animals receiving 3 mg/kg/week TVT-DOX were relatively stable throughout the treatment period, whereas the 1-mg/kg/week group showed

**Fig. 4**

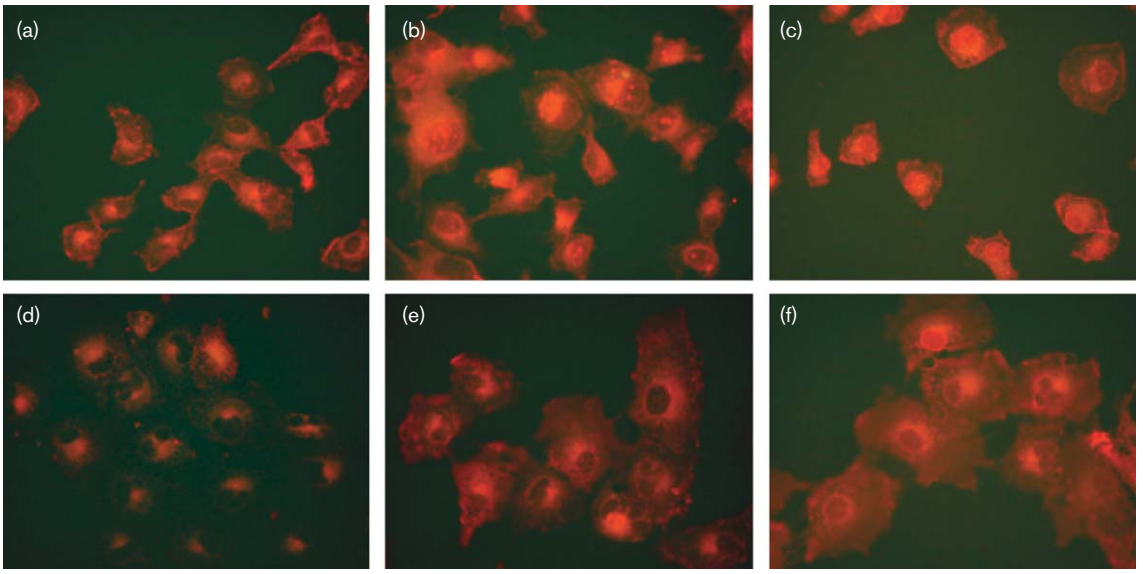


Kinetics of aspargine–glycine–arginine (NGR)-targeted liposomal doxorubicin (TVT-DOX) internalization in HT-1080 and Kaposi sarcoma-derived endothelial (SLK) cells: HT-1080 (a–c) and SLK (d–f) cells grown in chambered slides were incubated with TVT-DOX (20 μg/ml) for 15, 30 and 60 min at 37°C. The slides were washed, mounted and observed for DOX fluorescence. Original magnification × 500.

**Fig. 5**

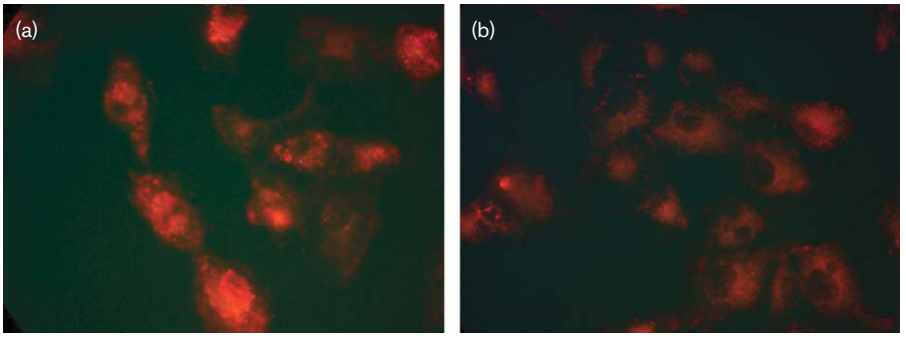


Bafilomycin A1 inhibits endosomal trafficking of aspargine–glycine–arginine (NGR)-targeted liposomal doxorubicin (TVT-DOX): Kaposi sarcoma-derived endothelial (SLK) cells grown in chambered slides were washed with phosphate-buffered saline (PBS) and preincubated at 37°C either in Hank's balanced salt solution (a) or 1 μmol/l bafilomycin (b) for 1 h; 20 μg/ml of TVT-DOX was then added and incubated for an additional 2 h. The cells were washed in PBS, mounted and observed for DOX fluorescence. Original magnification × 500.

no adverse effects of the drug (similar body-weight pattern as control group). This suggests that the 1- and 3-mg/kg/week doses of TVT-DOX were well tolerated when still showing efficacy in inhibiting the PC3-tumor growth.

To assess the effect of TVT-DOX on tumor blood vessels, we stained the cryosections of tumors from control and TVT-DOX-treated (6 mg/kg/week × 4) groups for CD31, a blood vessel marker. Our results indicate a pronounced destruction of blood vessels and a marked decrease in vessel density when comparing the TVT-DOX and control groups (Fig. 8d and e).

### *Colon-cancer HCT-116 model*

A comparison on the efficacy of TVT-DOX versus free DOX was made in the DOX-resistant colon-cancer model, HCT-116. Tumors in the vehicle-treated mice displayed typical growth characteristics and the first animal reached endpoint on day 28 (Fig. 9). DOX was marginally efficacious with treatment resulting in 30% growth inhibition, as calculated on day 28. TVT-DOX treatment

**Fig. 6**

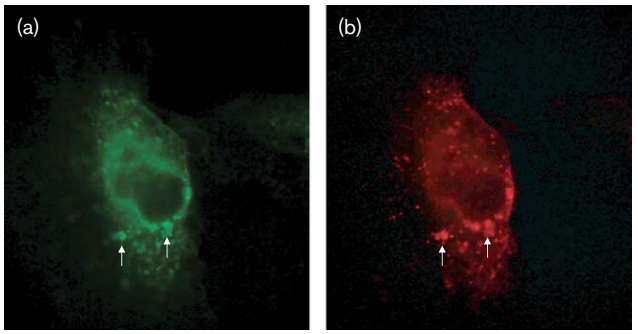


Colocalization of lysosomes and aspargine–glycine–arginine (NGR)-targeted liposomal doxorubicin (TVT-DOX): Kaposi sarcoma-derived endothelial (SLK) cells grown in chambered slides were washed with phosphate-buffered saline (PBS) and incubated simultaneously with Lyso Tracker Green DND-26 (a) and 20 μg/ml TVT-DOX (b) at 37°C in Hank's balanced salt solution for 1 h. The cells were washed in PBS, mounted and observed for fluorescence. The photomicrographs are of the same cell under fluorescein isothiocyanate (a) and triple-band pass (b) filters. Original magnification × 500.

(5 mg/kg/week × 5) showed significant growth inhibition (64%) compared with controls, on day 28 (Fig. 9). As depicted in Fig. 9, the first animal in the DOX group reached the endpoint on day 36, whereas in the TVT-DOX group it was on day 56. In summary, TVT-DOX treatment was superior to DOX in inhibiting HCT116 xenograft growth when administered intravenously at 5 mg/kg on a weekly schedule.

## Discussion

As the development of more efficacious and better tolerated anticancer drugs relies on the targeted delivery of therapeutic agents to tumor environments, the NGR-targeted liposomal DOX seemed attractive [21]. We further evaluated this drug for its in-vitro and in-vivo therapeutic efficacy following its scale-up preparation to suit the needs of future clinical development programs.

Our current investigations into the molecular targeting of TVT-DOX *in vitro* indicated specific binding and internalization of TVT-DOX in CD13-expressing tumor and endothelial cells. As mentioned earlier, only one isoform is believed to be the receptor for the NGR peptide and is exclusively present in tumor neovasculature [16,17]. As found by other groups, our findings of the TVT-DOX binding to endothelial cells (HUVEC and SLK) indicate that these cells express the tumor-specific CD13 isoform. Moreover, the binding of TVT-DOX to HT-1080 tumor cells suggests that some tumor types might also express the appropriate CD13 isoform and can be targeted with the same peptide. With both neovasculature and tumor cells being targeted, this will help to increase the therapeutic index of the drug.

**Fig. 7**

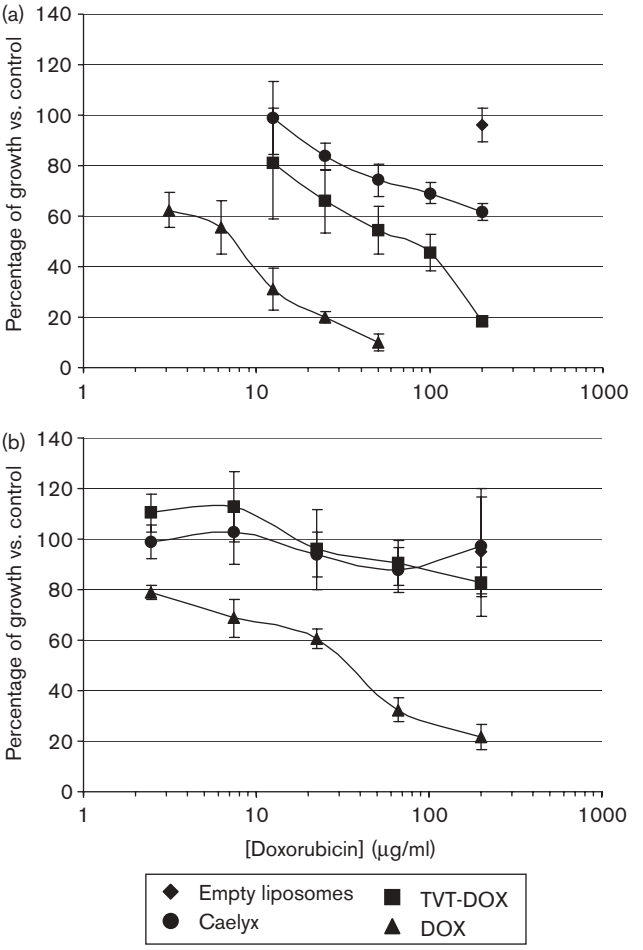


Enhanced cytotoxic effects of aspargine–glycine–arginine (NGR)-targeted liposomal doxorubicin (TVT-DOX) over Caelyx and its selectivity toward aminopeptidase N (CD13)-expressing cells. The CD13-positive human umbilical vein endothelial cells (a) and CD13-negative HT-29 cells (b) in monolayer culture were treated for 1 h with various DOX formulations at 37°C; the drugs were washed and cells were further incubated for 48 h in drug-free complete medium. Surviving cells were quantified by MTS assay.

The kinetics of drug uptake by cells, as observed by fluorescent microscopy, correlated with the degree of CD13 expression by the cells. The HT-1080 cells that expressed the most CD13 among the panel of studied cell lines in the current investigation were capable of internalizing the drug at a faster rate than the SLK cells. On these same cells, the binding and internalization of the nontargeted pegylated liposomal DOX was negligible within the tested incubation time. Taken together, this suggests an essential role of the NGR–CD13 association for cellular binding and internalization of liposomal DOX.

Cellular binding and internalization of liposomal DOX are unfortunately not a guarantee of the anticancer effect. It has been established that nuclear localization of DOX is

**Fig. 8**

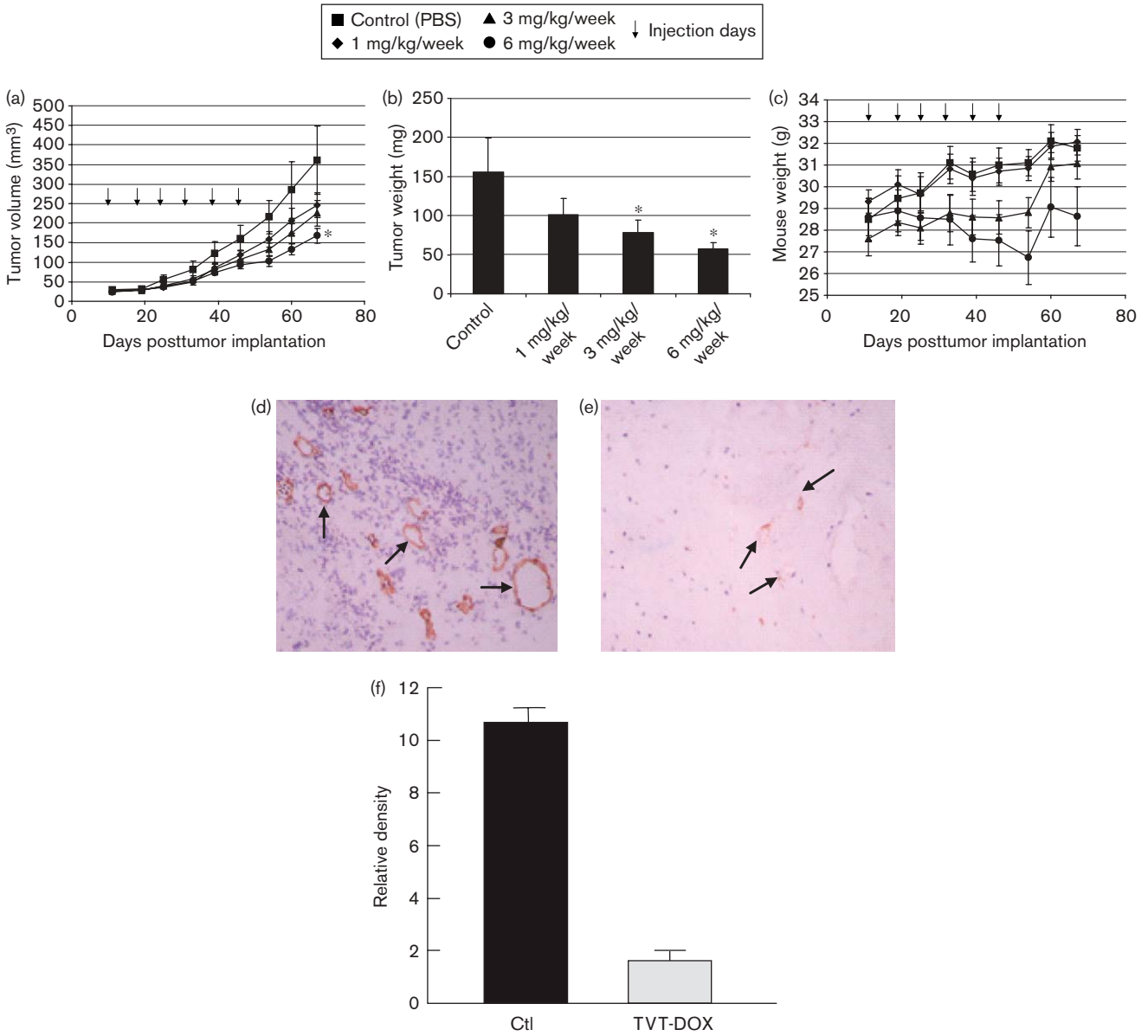


Suppressed PC3 xenograft growth in aspargine–glycine–arginine (NGR)-targeted liposomal doxorubicin (TVT-DOX)-treated nude mice: kinetics of PC3 tumor growth *in vivo* (a), PC3 tumor weight at termination (b), kinetics of mouse body weights (c), tumor-tissue sections immunostained for aminopeptidase N (CD31) to show blood vessels (indicated by ↑) in vehicle-treated control (d) and TVT-DOX-treated (e) animals. Original magnification × 200. *Significant differences between treated and control tumor-bearing animals Ctl, control and (f) quantification of blood vessel density was performed as described in Materials and Methods.

required for cell killing as it binds DNA and inhibits topoisomerase II [31]. In some cases, liposomal-encapsulated DOX is not as cytotoxic as one might predict, partly because of liposome stability once inside the cell [32]. Our histochemical results showed that, following a 1-h incubation at 37°C, the nontargeted liposomal DOX barely penetrated the cells and did not visibly enter the nucleus. In contrast, when it was associated with the NGR peptide, liposomal DOX readily entered the cell and was able to localize to the cell nucleus.

Bafilomycin A1 is an inhibitor of vacuolar-type $H^+$-ATPases involved in the acidification of endosomes [33]. The inhibition of perinuclear accumulation of liposomal drug in late endosomes and the nuclear uptake of DOX in bafilomycin-treated cells indicated that the acidic milieu of lysosome/endosomal vesicles was responsible for triggering the release of DOX from liposomes. It confirmed the endosomal trafficking of the drug in this investigation. The colocalization of Lyso Tracker Green and TVT-DOX in the same cellular area further lends

**Fig. 9**

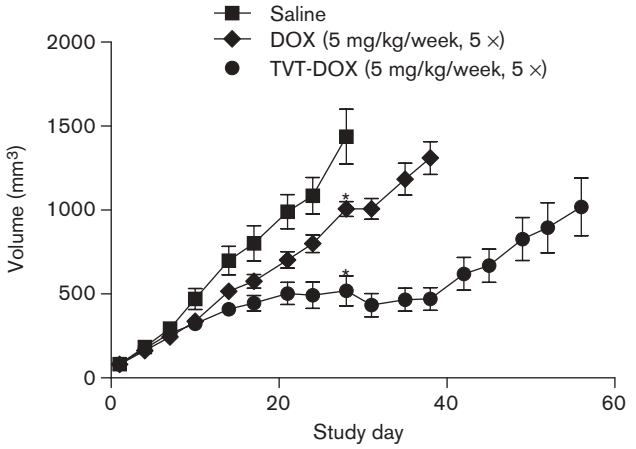


Enhanced antitumor effects of aspargine–glycine–arginine (NGR)-targeted liposomal doxorubicin (TVT-DOX) in the doxorubicin (DOX)-resistant colon-cancer HCT-116 xenograft model: kinetics of HCT-116 tumor growth in control, DOX-treated (5 mg/kg), and TVT-DOX-(5 mg/kg) animals. *Significant difference between treated and control tumor-bearing animals.

support to the localization of TVT-DOX in lysosome/endosomal vesicles.

The TVT-DOX quantitative-binding study results (Fig. 2b) seem to partially contradict the histologic observations (Figs 1b, f, j and n); when quantified, it seems that TVT-DOX binds to HT29 cells, whereas histologic analysis would suggest very limited drug binding. The contradiction might be due to the different sensitivity limits of the methods we used and might reflect a certain level of nonspecific binding of the TVT-DOX to the surface of any cell. The cytotoxicity results clearly show that CD13-positive HUVEC are more sensitive to the toxic effects of TVT-DOX than CD13-negative HT29 cells (Fig. 7). We hypothesize that there is a limited nonspecific binding of liposomes to the cells, but that the CD13-mediated interaction of targeted liposomes with the cells remains crucial for drug internalization and subsequent increased toxicity. Partial toxic effects of Caelyx on HUVEC might also be explained by the nonspecific binding of the liposomal formulation of DOX to the cells.

The selective TVT-DOX cytotoxicity in CD13-expressing HUVEC as opposed to CD13-negative HT-29 not only demonstrated the specificity for the drug toward CD13-expressing cells, but also confirmed that the cytotoxicity observed against HUVEC was not due simply to the leakage of DOX out of the liposomes. Although an assessment of free DOX in the two liposomal preparations indicated a slightly higher percentage in TVT-DOX (0.4%) than in Caelyx (0.2%), equivalent concentrations of free DOX did not elicit any cytotoxic effects in the same assay; this further confirmed that the enhanced cytotoxic effects of TVT-DOX were indeed due to the internalization of liposomal drug through the NGR peptide.

The in-vivo tumor-targeting properties of the NGR peptide have been reported previously by Arap *et al.* [12] and Ellerby *et al.* [18] in the breast-cancer model. Recently, it was reported that the addition of an NGR motif to human endostatin improved the inhibition of ovarian carcinoma growth [34]. In the DOX-resistant neuroblastoma mouse model, NGR-targeted liposomal DOX increased the survival time [21]. When testing this TVT-DOX formulation in a prostate-cancer model, we found it to be significantly effective in inhibiting PC3-tumor growth (Fig. 8a). Further, the destruction of tumor vascularization as noted by the reduced CD31 blood-vessel staining in treated animals confirmed the targeting of tumor neovasculature (Fig. 8e). Although the decrease in body weight at the highest dose of TVT-DOX (6 mg/kg) indicated some drug toxicity, the lower doses of TVT-DOX were well tolerated and still effective in inhibiting tumor growth. Additionally, any weight loss incurred during the treatment seemed reversible when drug administration ceased (Fig. 8c).

We also established the superiority of TVT-DOX in inhibiting the tumor growth over free DOX in the DOX-resistant HCT-116 colon-cancer model in this investigation. Although previous studies in a neuroblastoma model have already shown the advantage of targeting liposomal DOX with the NGR peptide [21], further studies to confirm the superiority of TVT-DOX over Caelyx are proposed for the HCT-116 model.

In-vivo activity in a tumor model of a particular histology does not always correlate with activity in the same human-cancer histology. The National Cancer Institute suggests that evidence of antitumor activity in multiple models is considered predictive of probable efficacy in human clinical trials [35]. To this effect, further studies on other tumor types and histologic origin are warranted to validate the in-vivo efficacy of TVT-DOX. The targeted delivery of DOX via NGR-liposomes might substantially improve the therapeutic index through the increased drug accumulation in the tumor, which would minimize systemic toxicities that are associated with free DOX [36].

## Acknowledgements

The following cell line was obtained through the AIDS Research and Reference Reagent Program, Division of AIDS, National Institute of Allergy and Infectious Diseases, National Institutes of Health: SLK cell line from Dr Sophie Leventon-Kriss.

## References


1 Matter A. Tumor angiogenesis as a therapeutic target. *Drug Discov Today* 2001; **6**:1005–1024.

2 Thorpe PE, Chaplin DJ, Blakey DC. The first international conference on vascular targeting: meeting overview. *Cancer Res* 2003; **63**:1144–1147.

3 Folkman J. Role of angiogenesis in tumor growth and metastasis. *Semin Oncol* 2002; **29**:15–18.

4 Jain RK. Molecular regulation of vessel maturation. *Nat Med* 2003; **9**:685–693.

5 Nicholson B, Schaefer G, Theodorescu D. Angiogenesis in prostate cancer: biology and therapeutic opportunities. *Cancer Metastasis Rev* 2001; **20**:297–319.

6 Brooks PC, Montgomery AM, Rosenfeld M, Reisfeld RA, Hu T, Klier G, *et al*. Integrin alpha v beta 3 antagonists promote tumor regression by inducing apoptosis of angiogenic blood vessels. *Cell* 1994; **79**:1157–1164.

7 Pasqualini R, Koivunen E, Kain R, Lahdenranta J, Sakamoto M, Stryhn A, *et al*. Aminopeptidase N is a receptor for tumor-homing peptides and a target for inhibiting angiogenesis. *Cancer Res* 2000; **60**:722–727.

8 Feng D, Nagy JA, Brekken RA, Pettersson A, Manseau EJ, Pyne K, *et al*. Ultrastructural localization of the vascular permeability factor/vascular endothelial growth factor (VPF/VEGF) receptor-2 (FLK-1, KDR) in normal mouse kidney and in the hyperpermeable vessels induced by VPF/VEGF-expressing tumors and adenoviral vectors. *J Histochem Cytochem* 2000; **48**:545–556.

9 Ruoslahti E. Specialization of tumour vasculature. *Nat Rev Cancer* 2002; **2**:83–90.

10 Chang SS, O'Keefe DS, Bacich DJ, Reuter VE, Heston WD, Gaudin PB. Prostate-specific membrane antigen is produced in tumor-associated neovasculature. *Clin Cancer Res* 1999; **5**:2674–2681.

11 Alessi P, Ebbinghaus C, Neri D. Molecular targeting of angiogenesis. *Biochim Biophys Acta* 2004; **1654**:39–49.

12 Arap W, Pasqualini R, Ruoslahti E. Cancer treatment by targeted drug delivery to tumor vasculature in a mouse model. *Science* 1998; **279**:377–380.

13 Zhang Z, Hatta H, Ito T, Nishimoto S. Synthesis and photochemical properties of photoactivated antitumor prodrugs releasing 5-fluorouracil. *Org Biomol Chem* 2005; **3**:592–596.

14 Zhang Z, Hatta H, Tanabe K, Nishimoto S. A new class of 5-fluoro-2′-deoxyuridine prodrugs conjugated with a tumor-homing cyclic peptide CNGRC by ester linkers: synthesis, reactivity, and tumor-cell-selective cytotoxicity. *Pharm Res* 2005; **22**:381–389.

15 O'Connell PJ, Gerkis V, d'Apice AJ. Variable *O*-glycosylation of CD13 (aminopeptidase N). *J Biol Chem* 1991; **266**:4593–4597.

16 Colombo G, Curnis F, de Mori GM, Gasparri A, Longoni C, Sacchi A, *et al*. Structure–activity relationships of linear and cyclic peptides containing the NGR tumor-homing motif. *J Biol Chem* 2002; **277**:47891–47897.

17 Curnis F, Arrigoni G, Sacchi A, Fischetti L, Arap W, Pasqualini R, *et al*. Differential binding of drugs containing the NGR motif to CD13 isoforms in tumor vessels, epithelia, and myeloid cells. *Cancer Res* 2002; **62**:867–874.

18 Ellerby HM, Arap W, Ellerby LM, Kain R, Andrusiak R, Rio GD, *et al*. Anti-cancer activity of targeted pro-apoptotic peptides. *Nat Med* 1999; **5**:1032–1038.

19 Grifman M, Trepel M, Speece P, Gilbert LB, Arap W, Pasqualini R, *et al*. Incorporation of tumor-targeting peptides into recombinant adeno-associated virus capsids. *Mol Ther* 2001; **3**:964–975.

20 Curnis F, Sacchi A, Borgna L, Magni F, Gasparri A, Corti A. Enhancement of tumor necrosis factor alpha antitumor immunotherapeutic properties by targeted delivery to aminopeptidase N (CD13). *Nat Biotechnol* 2000; **18**:1185–1190.

21 Pastorino F, Brignole C, Marimpietri D, Cilli M, Gambini C, Ribatti D, *et al*. Vascular damage and anti-angiogenic effects of tumor vessel-targeted liposomal chemotherapy. *Cancer Res* 2003; **63**:7400–7409.

22 Park JW, Hong K, Carter P, Asgari H, Guo LY, Keller GA, *et al*. Development of anti-p185HER2 immunoliposomes for cancer therapy. *Proc Natl Acad Sci U S A* 1995; **92**:1327–1331.

23 Saul JM, Annapragada A, Natarajan JV, Bellamkonda RV. Controlled targeting of liposomal doxorubicin via the folate receptor *in vitro*. *J Control Release* 2003; **92**:49–67.

24 Van Hensbergen Y, Broxterman HJ, Elderkamp YW, Lankelma J, Beers JC, Heijn M, *et al*. A doxorubicin-CNGRC-peptide conjugate with prodrug properties. *Biochem Pharmacol* 2002; **63**:897–908.

25 Allen TM, Hansen CB, de Menezes DEL. Pharmacokinetics of long-circulating liposomes. *Adv Drug Deliv Rev* 1995; **16**:267–284.

26 Coukell AJ, Spencer CM. Polyethylene glycol-liposomal doxorubicin. A review of its pharmacodynamic and pharmacokinetic properties, and therapeutic efficacy in the management of AIDS-related Kaposi's sarcoma. *Drugs* 1997; **53**:520–538.

27 Gabizon A, Martin F. Polyethylene glycol-coated (pegylated) liposomal doxorubicin. Rationale for use in solid tumours. *Drugs* 1997; **54 (Suppl 4)**: 15–21.

28 Gordon AN, Granai CO, Rose PG, Hainsworth J, Lopez A, Weissman C, *et al*. Phase II study of liposomal doxorubicin in platinum- and paclitaxel-refractory epithelial ovarian cancer. *J Clin Oncol* 2000; **18**:3093–3100.

29 Northfelt DW, Dezube BJ, Thommes JA, Levine R, von Roenn JH, Dosik GM, *et al*. Efficacy of pegylated-liposomal doxorubicin in the treatment of AIDS-related Kaposi's sarcoma after failure of standard chemotherapy. *J Clin Oncol* 1997; **15**:653–659.

30 Charrois GJ, Allen TM. Multiple injections of pegylated liposomal doxorubicin: pharmacokinetics and therapeutic activity. *J Pharmacol Exp Ther* 2003; **306**:1058–1067.

31 Taatjes DJ, Koch TH. Nuclear targeting and retention of anthracycline antitumor drugs in sensitive and resistant tumor cells. *Curr Med Chem* 2001; **8**:15–29.

32 Tseng YL, Liu JJ, Hong RL. Translocation of liposomes into cancer cells by cell-penetrating peptides penetratin and tat: a kinetic and efficacy study. *Mol Pharmacol* 2002; **62**:864–872.

33 Bayer N, Schober D, Prchla E, Murphy RF, Blaas D, Fuchs R. Effect of bafilomycin A1 and nocodazole on endocytic transport in HeLa cells: implications for viral uncoating and infection. *J Virol* 1998; **72**: 9645–9655.

34 Yokoyama Y, Ramakrishnan S. Addition of an aminopeptidase N-binding sequence to human endostatin improves inhibition of ovarian carcinoma growth. *Cancer* 2005; **104**:321–331.

35 Johnson JI, Decker S, Zaharevitz D, Rubinstein LV, Venditti JM, Schepartz S, *et al*. Relationships between drug activity in NCI preclinical *in vitro* and *in vivo* models and early clinical trials. *Br J Cancer* 2001; **84**:1424–1431.

36 Wallace KB. Doxorubicin-induced cardiac mitochondrionopathy. *Pharmacol Toxicol* 2003; **93**:105–115.